Proceedings of the 3rd International Conference on Computing Innovation and Applied Physics
DOI: 10.54254/2753-8818/26/20241003

Reliability analysis of single-story industrial buildings under wind load based on Monte Carlo simulation

Ruilin Qiu

College of Civil Engineering, Tongji University, Shanghai, 200082, China

qiuruilin@tongji.edu.cn

Abstract. Uncertain disasters such as typhoons can affect buildings. Single-storey industrial building is an important type of factory building. In this paper, the reliability of a single storey industrial building under wind load is studied by taking one typical factory in Hunan, China as an example. Firstly, finite element method is used to analyse the structure in the range of linear elasticity. Then, based on Monte Carlo simulation, the probability of failure of the structure under wind load is obtained. The results show that the probability of damage is relatively small, which is also in line with the fact that inland areas are not easily affected by typhoons. In order to obtain a deeper understanding of its reliability, the structural fragility curve considering the variability of steel strength is also studied. The results showed that the smaller the variability of the steel, the more beneficial it is for the reliability of the structure.

Keywords: Single-Story Industrial Building, Reliability Analysis, Wind Load, Monte Carlo Simulation.

1. Introduction

In China, single-story industrial buildings are widely used in heavy industries such as mechanical processing and metallurgy. The characteristic of this type of building is its large internal space, allowing large equipment and components to be transported within the factory. However, on the one hand, such buildings are highly susceptible to natural weather disasters such as typhoon. In 2015, Typhoon Mujigae passed through Zhanjiang, Guangdong. The walls and roof panels of a steel-framed industrial building were severely damaged. On the other hand, wind has significant uncertainty characteristics, so it is necessary to study it from a reliability perspective. Based on these two reasons, it can be seen that studying the reliability of single-story industrial buildings under wind load can help relevant personnel carry out building planning and renovation.

So far, a large number of methods have been applied to reliability assessment. Statistical inference techniques including Fault Tree Analysis (FTA) and Event Tree Analysis (ETA) can be used to evaluate reliability. However, to define the uncertainty of the dependence connection between various components or aspects of the assessed item, these approaches are sometimes challenging owing to the limited number of variables [1]. In order to solve the problems of traditional evaluation methods, techniques such as Bayesian Networks (BN), Monte Carlo simulations (MC), and Machine Learning (ML) have been used to analyse the structural reliability. Hackl and Kohler [2] proposed a reliability assessment method based on Dynamic Bayesian Networks (DBN), which is used to evaluate the degradation of concrete structures because of erosion. The study takes the parameters related to

DOI: 10.54254/2753-8818/26/20241003

corrosion and structure as nodes of BN, and the causal relationship between model parameters as edges of BN to construct the structure of BN. Zhou et al. [3] established a finite element model of a special-shaped double-layer continuous beam bridge and conducted nonlinear analysis under earthquake. At the same time, the MC simulation was applied to analyse the vulnerability of the bridge system. Dąbrowska [4] proposed a MC simulation for evaluating the reliability of aging complex multi-state technical systems and used it to estimate the reliability characteristics of port grain transportation systems.

It can be seen that the MC simulation has been widely applied due to its advantages such as simplicity, efficiency, randomness. Based on this, this research uses MC simulation to analyse the reliability of a single-story steel-framed industrial building in Hunan Province, China under wind load.

2. Methodology

2.1. Structural analysis based on numerical simulation

2.1.1. Project overview. The factory is a light steel structure located in Hunan Province, China. There are 3 spans in total, with each span of 18 meters. The longitudinal column spacing is 7.5 meters, with a total of 17 rigid frames. The foundation adopts the independent foundation under the column. Including the roof and purlins, the dead load of roof is 0.15 kN/m^2 and the live load is 0.30 kN/m^2. The reference wind pressure is 0.30 kN/m^2. The reference snow pressure is 0.30 kN/m^2. The beam and column of the rigid frame are H-shaped and made of Q345 steel. The roof purlins are Z-shaped cold-formed steel with inclined edges, using Q235 steel [5]. Figure 1 shows the structural layout.

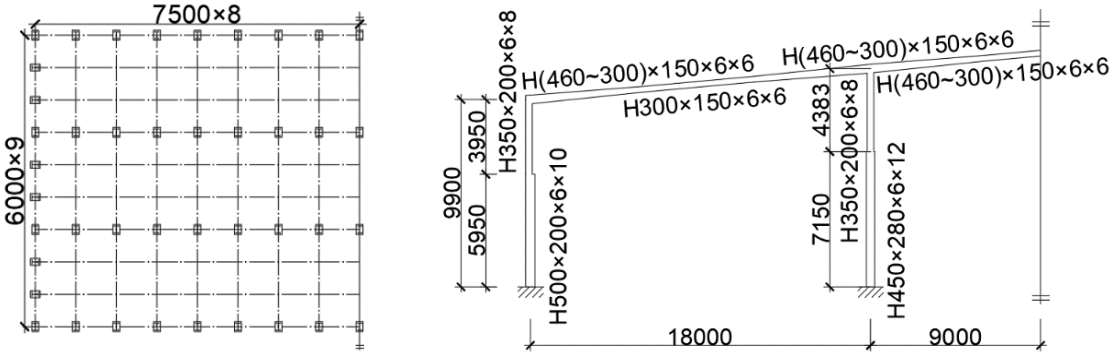

(a) Layout of column. (b) Parameters of the components.

Figure 1. Configuration of the structure.

2.1.2. Modelling and validation. In order to obtain the demand of the structure for use in subsequent MC simulation, it is necessary to use finite element software to analyse its internal forces. This study analyses the section stress under different load combinations and compares with that of the Zhang et al. [5]. Assuming the structure maintains linear elastic. The steel is an ideal elastic-plastic model with a yield strength of 345 N/mm^2. The element type is shell element S4R. The static general analysis step is used. The key sections of beam are shown in figure 2. The load combinations are shown in table 1, and the corresponding stress comparison results are shown in tables 2 to 5.

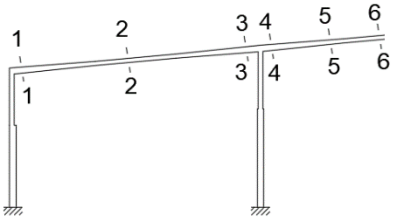

Figure 2. Key sections of steel beam.

DOI: 10.54254/2753-8818/26/20241003

Table 1. The load combination.

Label	Load combination
Combination 1	1.2*dead load+1.4*snow load
Combination 2	1.35*dead load+0.98*snow load
Combination 3	1.0*dead load+1.0*snow load
Combination 4	1.0*dead load+1.83*snow load

Table 2. Structural internal force of Combination 1.

Section position		1-1	2-2	3-3	4-4	5-5	6-6
Maximum principal stress (N/mm^2)	FEM	206	153	267	308	119	145
	Zhang et al.'s research [5]	195	166	270.6	301.2	120.8	145.2
	Error	0.3%	5.60%	7.80%	1.30%	2.30%	1.50%

Table 3. Structural internal force of Combination 2.

Section position		1-1	2-2	3-3	4-4	5-5	6-6
Maximum principal stress (N/mm^2)	FEM	166	123	222	277	111	140
	Zhang et al.'s research [5]	165.5	140.8	229.3	254.5	101.4	123.4
	Error	0.3%	12.6%	3.2%	8.8%	9.5%	13.5%

Table 4. Structural internal force of Combination 3.

Section position		1-1	2-2	3-3	4-4	5-5	6-6
Maximum principal stress (N/mm^2)	FEM	155	115	202	238	93.4	116
	Zhang et al.'s research [5]	147.4	125.4	204.5	227.4	91	109.8
	Error	5.2%	8.3%	1.2%	4.7%	2.6%	5.6%

Table 5. Structural internal force of Combination 4.

Section position		1-1	2-2	3-3	4-4	5-5	6-6
Maximum principal stress (N/mm^2)	FEM	243	180	306	331	126	146
	Zhang et al.'s research [5]	222.7	189.5	309.3	345	139.1	165.4
	Error	9.1%	5.0%	1.1%	4.1%	9.4%	11.7%

From tables 2-5, it can be seen that except for a few cases, most errors are within 10%. The sections with significant error mainly appear in section 2-2 and 6-6. The main reasons for this are analysed as follows. During the calculation, it was found that there were significant torsional and out of plane bending effects in the members, which were particularly evident in the beam segments far from the column ends (i.e., section 2-2 and 6-6).

Considering there are purlins, roof panels, and crane beams restraining the out-of-plane deformation in practical engineering, out-of-plane constraints are also applied in the model. However, corresponding stress would also be generated. Meanwhile, even if some relative errors exceed 10%, the difference in absolute values does not exceed 20 MPa. Therefore, the author believes that the results of validation model are acceptable. The model can be used for structural analysis of subsequent wind loads.

2.1.3. Structural internal force analysis under wind load. Based on the Chinese code, the wind load on the single-story industrial building is shown in figure 3 [6].

DOI: 10.54254/2753-8818/26/20241003

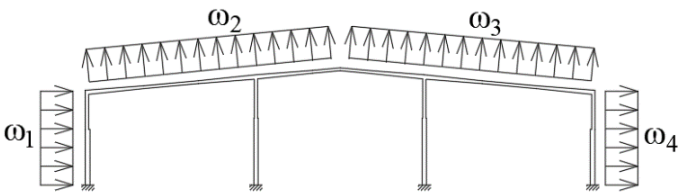

Figure 3. Load diagram.

The ω_i can be calculated through equation (1).

$$\omega_i = \frac{\mu_{si} \cdot \mu_{zi} \cdot w}{f_i} \omega_0 \quad i=1,2,3,4 \tag{1}$$

where,

μ_{si} is shape coefficient of wind pressure. μ_{s1}=0.8, μ_{s2}=0.6, μ_{s3}=0.5, μ_{s4}=0.5;

μ_{zi} is height coefficient of wind pressure. $\mu_{z1}=\mu_{z4}$=1.0, $\mu_{z2}=\mu_{z3}$=1.13;

w is the width of the enclosure wall allocated by one rigid frame (m);

f_i is the width of flange (mm), $f_1=f_4$=200mm, $f_2=f_3$=150mm;

ω_0 is reference wind pressure (N/mm^2)

A finite element model is established based on this model. Considering that the wind load shown in figure 3 does not have symmetry, the other half of the validation model is supplemented completely. Von Mises yield criterion is adopted, and the Von Mises stress equation is:

$$S = \sqrt{\frac{1}{2}[(\sigma_1-\sigma_2)^2+(\sigma_2-\sigma_3)^2+(\sigma_3-\sigma_1)^2]} \tag{2}$$

where $\sigma_1, \sigma_2, \sigma_3$ are first, second, third principal stress, respectively.

2.2. Reliability analysis based on MC simulation

2.2.1. Distribution of wind load. The reference wind pressure is an uncertain quantity, therefore determining the reference wind pressure ω_0 is necessary. The relationship between reference wind pressure ω_0 and reference wind speed v_0 can be calculated according to equation (3):

$$\omega_0 = \frac{1}{2}\rho v_0^2 \tag{3}$$

where v_0 is reference wind speed (m/s), and ρ is density of air, which is equal to 1.29kg/m^3.

Therefore, the problem is transformed into determining the distribution of reference wind speed. According to the code, the statistical sample of wind speed should adopt the annual maximum value and Gumbel Distribution [6]. The Cumulative Distribution Function (CDF) and Probability Density Function (PDF) are shown in equations (4) and (5), respectively.

$$F(x) = e^{-e^{-\alpha(x-u)}} \tag{4}$$

$$f(x) = \alpha e^{-\alpha(x-u)-e^{-\alpha(x-u)}} \tag{5}$$

where,

α is scale parameter;

u is location parameter;

γ = 0.5772156649⋯ is Euler's constant.

The wind load samples were obtained through the database provided by the Global Hourly - Integrated Surface Database (ISD) website [7]. The annual maximum wind speed recorded at Chenzhou

DOI: 10.54254/2753-8818/26/20241003

(NO. 57972 Station) in Hunan Province for a total of 10 years from 2013 to 2022 was selected, and the annual maximum wind pressure was calculated, as shown in table 6. After that the mean and standard deviation of the sample can be obtained. Then two parameters of Gumbel Distribution can be obtained. Finally, the PDF and CDF of the reference wind pressure can be obtained, as shown in figures 4 and 5.

Table 6. Annual maximum wind speed and pressure at Chenzhou Station in Hunan from 2013 to 2022.

Year	Annual maximum wind speed (m/s)	Annual maximum wind pressure (N/mm^2)
2013	7	31.61
2014	6	23.22
2015	6	23.22
2016	16	165.12
2017	16	165.12
2018	17	186.41
2019	16	165.12
2020	15.7	158.99
2021	14.5	135.61
2022	15	145.13

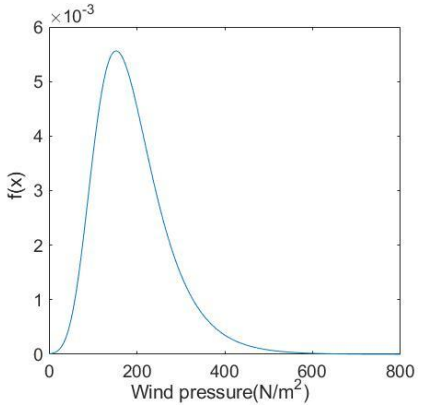

Figure 4. Probability density function.

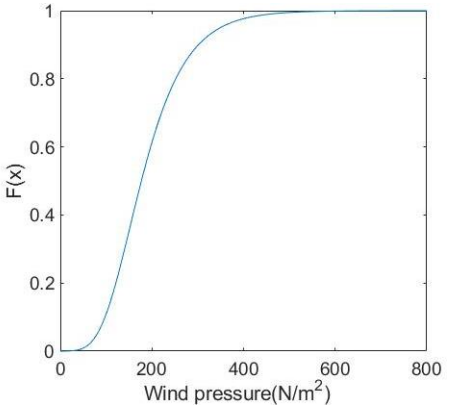

Figure 5. Cumulative distribution function.

The reference wind pressure specified in the code for this area is 300N/mm^2. According to the definition of reference wind pressure, in most cases, the wind pressure should be less than 300N/mm^2. It can be seen that F(300)=0.8978 from figure 5, which meets the reference wind pressure defined by the specification. Therefore, this statistical result is reasonable.

2.2.2. Probability of failure. The possibility that a structure will carry out its intended function within a given time frame and under a set of conditions is known as structural reliability [8]. The probability of a structure being in a failure state is called probability of failure (POF), expressed as p_f. If the load effect and resistance of the structure are defined as D and C respectively, then:

$$p_f=P\{C<D\} \tag{6}$$

The goal of MC simulation is using random numbers with one specific distribution to replicate random occurrences that could happen in real systems. Due to the fact that every simulation test can merely describe one possible occurrence of the system under consideration, valuable statistical

DOI: 10.54254/2753-8818/26/20241003

conclusions can be drawn after conducting a quantity of tests, based on the central limit theorem and large number theorem of probability theory [9]. Based on MC simulation, POF can be computed through MATLAB programming. The algorithm flowchart is shown in figure 6.

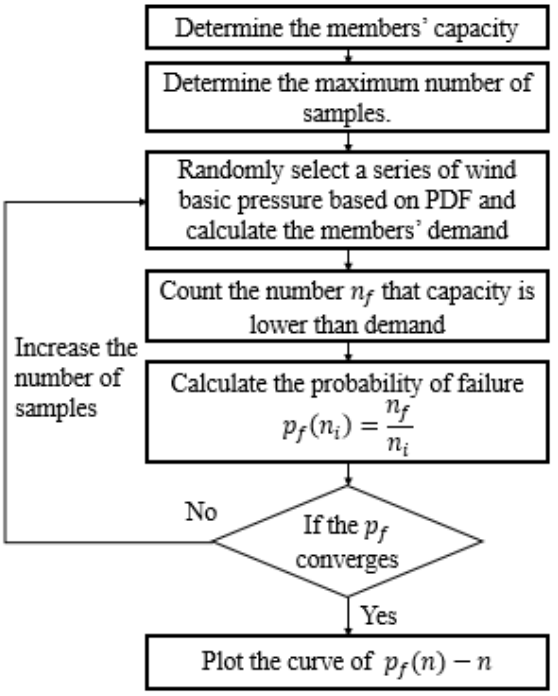

Figure 6. Flowchart for calculating the probability of failure.

2.2.3. Fragility of structure. The fragility curve is a precise and quantitative fragility evaluation method and a key link in disaster assessment. Its core element is to express the quantitative relationship between the intensity of hazard factors and the fragility of disaster-bearing bodies.

In practical engineering, due to limitations in processing and construction techniques, the material of the structure has significant uncertainty [10]. Therefore, this section studies the POF under different reference wind pressure when considering material uncertainty, and draws corresponding fragility curves. Zhai et al. [11] recorded the strength of a batch of steel from a factory in Shanghai, China. Assuming the yield strength of steel follows a lognormal distribution. The mean of the steel sample is 345N/mm^2. Referring to the results of the paper, the variance is set to 595N^2/mm^4. Then, the two parameters of the lognormal distribution can be calculated according to equation (7), λ= 5.8411, ξ= 0.0706.

$$\begin{cases} \lambda = \ln \dfrac{\mu^2}{\sqrt{\sigma^2 + \mu^2}} \\ \xi = \sqrt{\ln \dfrac{\sigma^2}{\mu^2} + 1} \end{cases} \tag{7}$$

The algorithm flowchart is shown in figure 7. Fragile curves can be obtained by MATLAB programming.

DOI: 10.54254/2753-8818/26/20241003

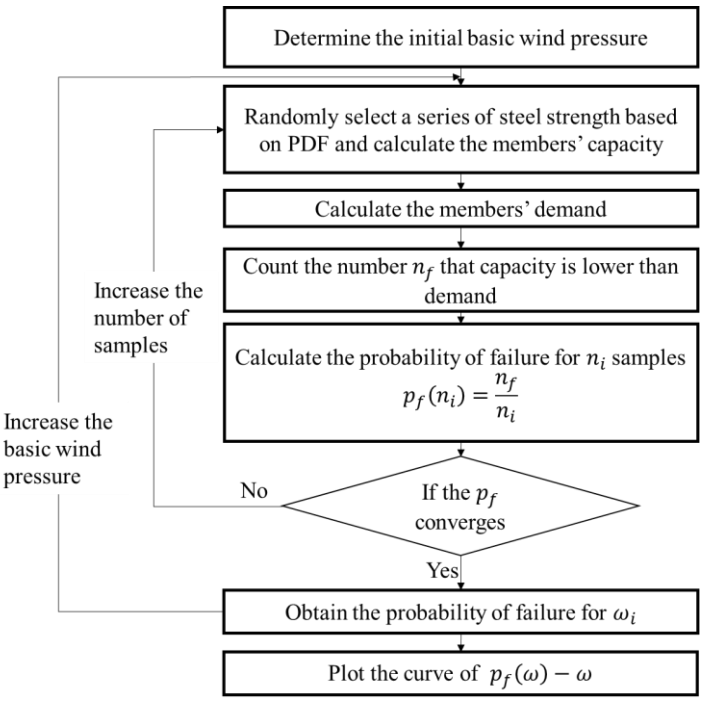

Figure 7. Flowchart for calculating the fragility.

3. Results

3.1. Structural internal force results and discussion

Through finite element analysis, the Mises stress cloud diagram of the rigid frame can be obtained (ω_0=1), as shown in figure 8. It can be concluded that the dangerous sections of the rigid frame should mainly be concentrated at the beam end, mid span of the beam, and column end. This is consistent with the cloud diagram obtained from finite element analysis, which can indicate that the finite element results are reasonable. The dangerous section of the rigid frame is shown in figure 9. The corresponding stress is shown in table 7.

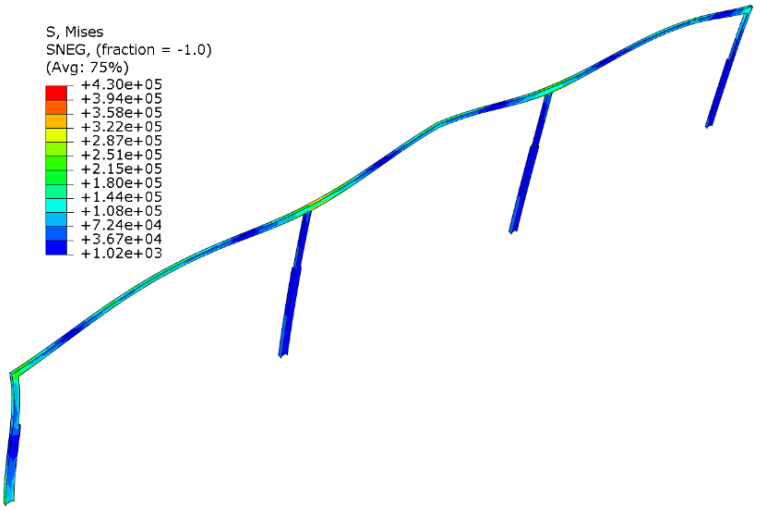

Figure 8. Mises stress cloud diagram of rigid frame.

DOI: 10.54254/2753-8818/26/20241003

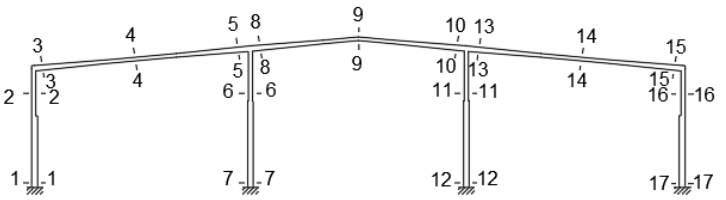

Figure 9. Dangerous sections of the rigid frame.

Table 7. Mises stress of dangerous sections.

Section number	Mises stress
1-1	$226700\omega_0$
2-2	$241900\omega_0$
3-3	$269200\omega_0$
4-4	$166800\omega_0$
5-5	$270000\omega_0$
6-6	$62500\omega_0$
7-7	$50200\omega_0$
8-8	$368400\omega_0$
9-9	$408400\omega_0$
10-10	$363800\omega_0$
11-11	$83600\omega_0$
12-12	$54000\omega_0$
13-13	$273900\omega_0$
14-14	$141800\omega_0$
15-15	$182500\omega_0$
16-16	$147300\omega_0$
17-17	$47700\omega_0$

It can be observed that with the ω_0 increases, the internal force of the structure will also increase linearly within the linear elastic range. As the structure is statically indeterminate, yielding at one certain section will not result in structural failure. Along with ω_0 increases, the three sections of 9-9, 8-8, and 10-10 will yield in priority, meaning that the beam in the middle span will fail first, which is considered structural failure. Therefore, when the 10-10 section yields, it is determined as structural failure.

3.2. Reliability results and discussion

3.2.1. Analysis of probability of failure. Based on the flowchart in section 2.2.2, the POF curve can be obtained, as shown in figure 10. It can be found that:

(1) After collecting enough samples, the POF tends to stabilize at 3.58×10^{-4}. As Hunan is located in the inland of China, it is less affected by typhoon weather. As long as the building design and construction meet the restrictions of design specifications, safety can be basically ensured. However, in recent years, there have also been occasional extreme weather events, resulting in a small probability of structural failure. In addition, this study only focuses on structural components and does not conduct

DOI: 10.54254/2753-8818/26/20241003

research on non-structural components. Therefore, it is not ruled out that non-structural components may have a high POF under wind disasters. Therefore, the result of this POF is relatively reasonable.

(2) Additionally, MC simulation is not suitable for situations where POF is extremely low. Taking POF of this project as an example, less than 4 out of 10000 samples are considered to have failed. If the sample size is too small, there will be serious discrete problems. Therefore, in order to obtain good convergence results, a large number of samples are required (in this case, a maximum of 30000 samples were used, and the program went through approximately 450 million cycles). However, it also resulted in a long analysis time.

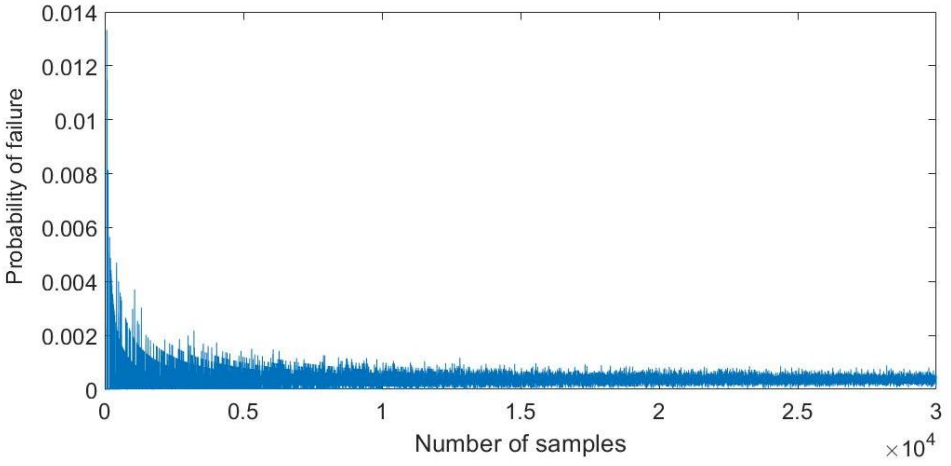

Figure 10. Probability of failure curve of structure.

3.2.2. Analysis of structural fragility. Based on the flowchart in section 2.2.3, the fragility curve can be obtained, as shown in figure 11. It can be observed that when the reference wind pressure is less than 0.55kN/m^2, the POF is still close to 0 even though considering material uncertainty. The result indicates that the structure has sufficient redundancy. As the reference wind pressure increases, POF gradually increases. When reference wind pressure reaches 0.85kN/m^2, the POF is close to 1.

At the same time, this study further investigated the impact of uncertainty in structural materials on fragility, and analysed the impact of steel strength on the fragility curve under different variance, as shown in figure 12. As the variance decreases, the rising segment of the fragile curve becomes steeper, and the starting point of the rising segment shifts back. It helps to improve the reliability of the structure, although this improvement is not very obvious.

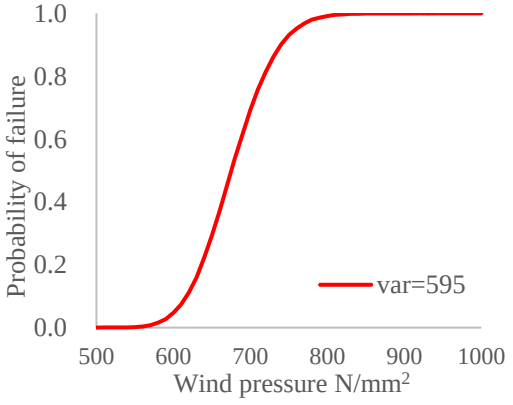

Figure 11. Fragility curve of structure.

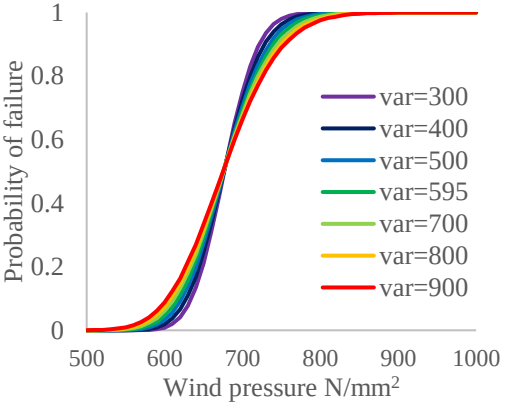

Figure 12. Fragility curves of steel strength under different variances.

DOI: 10.54254/2753-8818/26/20241003

4. Conclusion

In order to study the reliability of single-story industrial buildings under wind load, this study focuses on analysing the force characteristics of a steel structure factory building in Hunan Province under wind load. The internal force and main failure modes within the linear elastic range are obtained through finite element analysis. In addition, this study introduces the MC method to simulate the POF and fragility curve of structure. It is found that the POF of the building is relatively low, which is in line with the actual situation that the building is situated inside the mainland and less susceptible to typhoon disasters.

However, there are some shortcomings in this study. Firstly, as mentioned earlier, MC simulation is not suitable for analysing situations with low POF. When POF is low, the convergence speed will be slow, resulting in high computational costs. In the future, it is necessary to find new methods or continue to improve MC methods to avoid discreteness and convergence issues. In addition, this study has not considered the uncertainty of geometric dimensions or structural construction, which leads to the inaccuracy of the fragility curve. Further research is needed on structural fragility analysis under various uncertain factors.

References

[1] Bobbio A, Portinale L, Minichino M and Ciancamerla E 2001 Improving the analysis of dependable systems by mapping fault trees into Bayesian networks *Reliability Engineering & System Safety* 71(3) 249-260

[2] Hackl J and Kohler J 2016 Reliability assessment of deteriorating reinforced concrete structures by representing the coupled effect of corrosion initiation and progression by Bayesian networks *Structural Safety* 62 12-23

[3] Zhou Y, Wang W, Lv X and Cheng Y 2023 Seismic vulnerability analysis of special－shaped double-layer continuous beam bridge based on Monte－Carlo method *Earthquake Resistant Engineering and Retrofitting* 45(4) 100-107+117

[4] Dąbrowska E 2020 Monte Carlo Simulation Approach to Reliability Analysis of Complex Systems *Journal of KONBiN* 50(1) 155-170

[5] Zhang W, Yi W, Xiao Y and Wu Y 2014 Collapse simulation and robustness analysis of a certain one-story steel industrial factory building during snow disaster *Industrial Construction* 44(1) 154-159

[6] *Load code for the design of building structures: GB 50009-2012* 2012 Beijing: Ministry of Housing and Urban-Rural Development of the People's Republic of China

[7] Integrated Surface Database (ISD) 2023 *https://www.ncei.noaa.gov/products/land-based-station/integrated-surface-database*

[8] Li G, Huang H, Wu X, Liu S and Sun F 2016 *Principles of Load and Reliability Design for Engineering Structures* vol 4, ed W Ji and S Zhu (Beijing: China Architecture & Building Press) pp 143-144

[9] Yang H 2004 *Application research on Monte Carlo simulation and optimization of decision analysis under risk* Tianjin University

[10] Baji H 2014 *The effect of uncertainty in material properties and model error on the reliability of strength and ductility of reinforced concrete members* University of Queensland

[11] Zhai J, Li J and Wang S 1992 Statistical analysis for strength variance of structural steel *Journal of Taiyuan Heavy Machinery Institute* 13(1) 104-108